

## Determining of variables influencing soil organic carbon content of PNR-Cortadera paramo (Colombia) via remote sensing

Determinación de variables que influyen en el contenido de carbono orgánico del suelo del páramo PNR-Cortadera (Colombia) mediante teledetección

PABLO CESAR SERRANO-AGUDELO<sup>1,5</sup>

LUIS JOEL MARTÍNEZ-MARTÍNEZ<sup>2</sup>

PABLO ANTONIO SERRANO-CELY<sup>3</sup>

ADRIANA BOLÍVAR-GAMBOA<sup>4</sup>

DIEGO FERNANDO MORENO-PÉREZ<sup>4</sup>

<sup>1</sup> Unidad de Planificación Rural Agropecuaria, Bogota (Colombia). ORCID Serrano-Agudelo, P.C.:

<https://orcid.org/0000-0002-2563-2050>

<sup>2</sup> Universidad Nacional de Colombia, Facultad de Ciencias Agrarias, Bogota (Colombia). Martínez-Martínez, L.J.: <https://orcid.org/0000-0001-9010-9189>

<sup>3</sup> Universidad Pedagógica y Tecnológica de Colombia, Facultad de Ciencias Agropecuarias, Grupo de investigación GIPSO, Tunja (Colombia). ORCID Serrano-Cely, P.A.: <https://orcid.org/0000-0002-1270-3024>

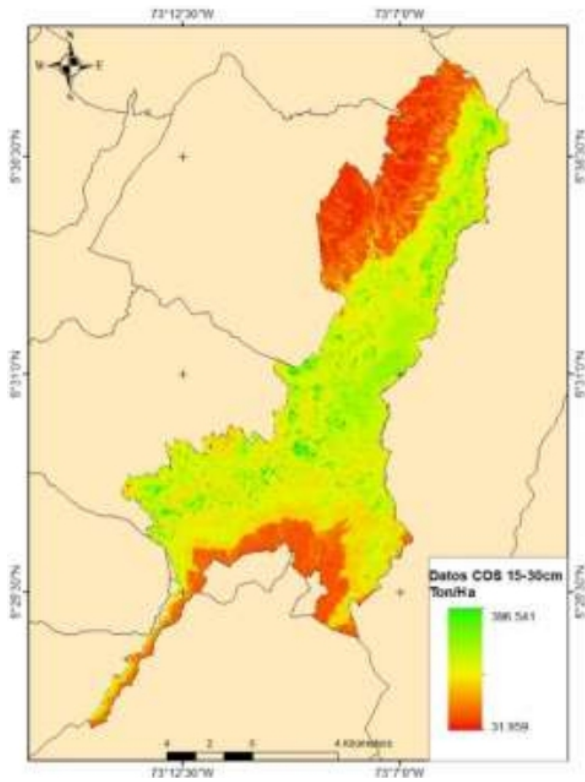
<sup>4</sup> Investigador Independiente, Tunja (Colombia). ORCID Bolívar-Gamboa, A.: <https://orcid.org/0000-0002-5167-0958>; ORCID Moreno-Pérez, D.F.: <https://orcid.org/0000-0002-1688-3771>

<sup>5</sup> Corresponding authors. [pcsserranoa@gmail.com](mailto:pcsserranoa@gmail.com)

**Last name:** SERRANO-AGUDELO / MARTÍNEZ-MARTÍNEZ / SERRANO-CELY / BOLÍVAR-GAMBOA / MORENO-PÉREZ

**Short title:** SOIL ORGANIC CARBON IN LA CORTADERA PÁRAMO

**Doi:** <https://doi.org/10.17584/rcch.2024v18i2.17464>



**Estimation of soil organic carbon at 15 to 30 cm depth.**

Source: P.C. Serrano-Agudelo

## ABSTRACT

The soil organic carbon (SOC) content under climate change scenarios is essential, especially in areas of difficult access such as the high-altitude Tropical paramos. This study aimed to correlate the digital elevation model (DEM) derivatives, spectral indices from Sentinel-1 and Sentinel-2, and WorldClim data with *in situ* SOC content in the PNR-Cortadera paramo (Boyaca, Colombia). Based on 169 soil samples collected at two depths (0-15 and 15-30 cm) organic carbon was determined using the Walkley-Black method. SOC contents ranged from 25 to 200 t HA-1 at 0-15 cm and from 33 to 466 t ha<sup>-1</sup> at 15-30 cm. Altitude, temperature, NDVI, TWI<sub>0-15 cm</sub>, MRVBF, LS factor<sub>0-15 cm</sub> and VH band polarization showed the highest correlations and the lowest variance inflation factor. The highest SOC contents are located in the central and southern area of the paramo due to the higher altitude, greater precipitation and presence of vegetation cover.

**Additional keywords:** soil recognition; High tropics; climate change; carbon dioxide capture and storage; remote sensing.

## RESUMEN

El contenido de carbono orgánico (COS) del suelo bajo escenarios de cambio climático es esencial, especialmente en áreas de difícil acceso como los páramos tropicales de gran altitud. Este estudio tuvo como objetivo correlacionar los derivados del modelo de elevación digital (DEM), los índices espectrales Sentinel-1 y Sentinel-2 y los datos de WorldClim con el contenido de COS *in situ* en el páramo PNR-Cortadera (Boyacá, Colombia). A partir de 169 muestras de suelo recolectadas a dos profundidades (0-15 y 15-30 cm), se determinó el carbono orgánico mediante el método de Walkley-Black. Los contenidos de COS a 0-15 cm de profundidad variaron entre 25 a 200 t ha<sup>-1</sup> y 33 a 466 t ha<sup>-1</sup> a 15-30 cm. La altitud, la temperatura, el NDVI, el TWI<sub>0-15 cm</sub>, el MRVBF, el factor LS<sub>0-15 cm</sub> y la polarización de la banda VH mostraron las mejores correlaciones y el menor factor de inflación de la varianza. Los mayores contenidos de COS se ubican en la zona central y sur del páramo debido a la mayor altitud, precipitación y presencia de cobertura vegetal.

**Palabras clave adicionales:** reconocimiento del suelo; Trópicos altos; cambio climático; captura y almacenamiento de dióxido de carbono; teledetección.

## INTRODUCTION

Paramos are unique high-altitude tropical ecosystems characterized by their distinctive vegetation, prevailing climate conditions, soils, and altitudinal ranges (Morales *et al.*, 2007). They are strategic as they provide ecosystem services such as water supply, carbon capture by vegetation, and soil organic matter retention (Africano *et al.*, 2016).

Soils can retain about three times more carbon than terrestrial plant and animal biomass and twice the carbon contained in the atmosphere (Reyes *et al.*, 2018; Andrade *et al.*, 2022). Paramo soils accumulate carbon due to low temperatures and the slow decomposition of plant residues (Ayala *et al.*, 2014), which is of great relevance in scenarios of mitigation and adaptation to the negative effects associated with climate change, as they sequester more carbon than many other ecosystems (Zimmermann *et al.*, 2010).

The Kyoto Protocol recognizes that net greenhouse gas emissions can be reduced either by decreasing the emission rate into the atmosphere or by increasing the removal rate by carbon sinks (FAO, 2017). To mitigate greenhouse gases, an agreement was created between countries for the trading of carbon credits. A carbon credit corresponds to the equivalent of one ton of carbon dioxide (t CO<sub>2</sub> eq) removed from the atmosphere.

Since the first quarter of 2016, Colombia has implemented negotiations under the administration of the Agricultural Commodity Exchange, aiming to reduce 500,000 t CO<sub>2</sub> eq (Cuervo-Barahona *et al.*, 2016). Based on this, understanding the SOC content of paramo soils and their spatial and temporal dynamics could highlight the function of this ecosystem in mitigating the effects of climate change and justify the adoption of economic incentives in the management of natural resources (Ward *et al.*, 2016).

Soil organic carbon (SOC) is an important component of the global carbon cycle, representing 69.8% of the carbon in the biosphere (FAO, 2017; Andrade *et al.*, 2022). It plays a significant role because, depending on land use and management, it can act as either a source or reservoir of carbon (Huamán-Carrión *et al.*, 2021; Canaza *et al.*, 2023). Soils act as carbon reservoirs or emitters depending on several factors. Changes in SOC content in the top centimeters of soil result from modifications in land cover. For example, changing native vegetation to agricultural soils causes SOC losses, generating greenhouse gas (GHG) emissions that contribute to climate change (Burbano, 2018). Additionally, rising temperatures can increase GHG emissions. Topography and soil type also directly influence carbon storage. Soil moisture content resulting from climatic conditions affects microbial activity and thus the decomposition of organic materials (Carrillo-Rojas *et al.*, 2019).

Reports on SOC in paramo ecosystems are scarce, focusing on changes in carbon content due to different land cover uses (Montes-Pulido *et al.*, 2017; Barrezueta-Unda *et al.*, 2019; Andrade *et al.*, 2022). Moreno *et al.* (2017) emphasize differences in SOC content at 4 m depth among primary, secondary, and pasture forests. Additionally, geomorphology and management practices are crucial in SOC dynamics (Lis-Gutiérrez *et al.*, 2019), with SOC estimation strongly associated with precipitation, temperature, altitude, and organic matter content (Canaza *et al.*, 2023). In situ studies of these ecosystems are challenging due to their heterogeneity and remoteness, complicating field information collection (Ayala *et al.*, 2019). This makes remote sensing a promising alternative as it provides a wealth of information through spectral indices, topographical elements, geological features, soil taxonomy, and climate data.

Given the importance of understanding SOC distribution in paramo ecosystems, which provide essential ecosystem services such as water retention and distribution, act as carbon sinks, and support diverse communities, the objective of this research was to correlate available information from remote sensors (DEM Alos Palsar), Sentinel 1 and 2 spectral indices, and WorldClim climate data with SOC content in the La Cortadera paramo from in situ samples.

## MATERIALS AND METHODS

The study area encompassed the *Parque Natural Regional* PNR-Cortadera (<https://www.corpoboyaca.gov.co/sirap/?s=de+p%C3%A1ramo>), a protected area within the Tota-Bijagual-Mamaciha paramo complex. This complex covers an area of 16,508.4 ha, with an altitudinal range of 2,350-3,850 m, and vegetation cover ranging from Andean High Forest to Paramo. It serves as a recharge source for the La Copa reservoir, supplying the Pesca, Jordan, Tuta, Salitre, and Muche rivers, and forming part of the Chicamocha and Upia river basins, and provides water for municipal and rural water supply systems. The temperature ranges from 6 to 12°C, and precipitation from 500 to 1,000 mm year<sup>-1</sup> (Morales *et al.*, 2007; Corporinoquia, 2017).

A total of 169 soil samples were collected from six georeferenced transects during two sampling periods (2017 and 2020). Samples from two depths (0-15 cm and 15-30 cm) were analyzed to determine the percentage of carbon (C) using the Walkley-Black method (wet oxidation). Soil organic carbon content was estimated in tons (Gardi *et al.*, 2014) using the following equation (1) (Rügnitz *et al.*, 2009)

$$SOC = C \times \rho b \times Depth \times (1 - frag) \times 10 \quad (1)$$

where *SOC* was the soil organic carbon content (t ha<sup>-1</sup>), *C* the determined organic carbon concentration, *ρb* the bulk density, *Depth* the depth of the soil horizon or thickness of the soil layer (m), and *Frag* the volume percentage of coarse fragments/100.

The Sentinel-1 image, taken on June 28, 2017, was processed with SNAP. The image was calibrated with the Sigma incidence angle to obtain square pixels, the multilooking filter was applied to two ranges, and the noise was corrected with the Lee Sigma filter in a 7×7 window. Alos-Palsar was used for the correction, and the digital level values were converted to values of backscatter on the decibel scale, with VV-VH polarimetric data used as covariates.

From an orthorectified BoA Sentinel-2A image from January 17, 2019 and corrected with Sen2Cor, spectral indices were obtained, including the Normalized Difference Vegetation Index (NDVI), Enhanced Vegetation Index (EVI), Bare Soil Index (BSI), Advanced Vegetation Index (AVI), Soil Adjusted Vegetation Index (SAVI), Green Normalized Difference Vegetation Index (GNDVI), Normalized Difference Moisture Index (NDMI), Moisture Stress Index (MSI), Normalized Difference Water Index (NDWI), and Normalized Burn Ratio Index (NBRI).

The Alos Palsar DEM digital elevation model had a spatial resolution of 12.5 m and was radiometrically corrected by the Alaska Satellite Facility. It provided derivatives such as altitude, slope,

flow direction, flow accumulation, aspect, curvature, Multiresolution Index of Valley Bottom Flatness (MRVBF), Multiresolution Index of the Ridge Top Flatness (MrRTF), Topographic Wetness Index (TWI), and slope length and steepness factor (LS-factor).

Precipitation and temperature data were obtained from the WorldClim platform, version 2.1 published in 2020, corresponding to the period 1970-2000, with a resolution of 30 arc-seconds (the maximum available). The data from this platform are calibrated with meteorological station data. The multi-annual average temperature and precipitation were used.

### Statistical analysis

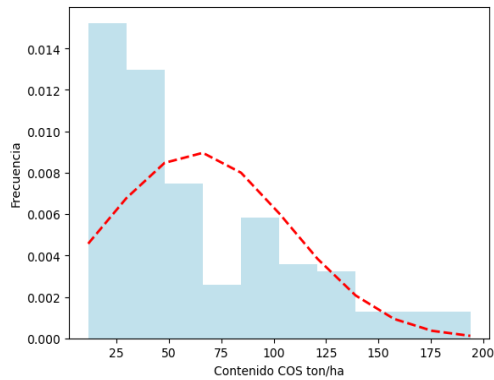
The Pearson correlation coefficient was calculated for the relationship between the SOC contents and the information from remote sensing systems. The variance inflation factor (VIF) (Zuur *et al.*, 2007) was also calculated to establish statistical redundancy and collinearity. Based on the resulting values and according to Armas *et al.* (2017), variables with lower VIF and higher correlation coefficients were selected.

## RESULTS AND DISCUSSION

SOC contents at a depth of 0-15 cm were grouped into three categories (Fig. 1A), with the largest proportion of values being less than 50 t ha<sup>-1</sup>, a smaller proportion between 50 and 150 t ha<sup>-1</sup>, and few above 150 t ha<sup>-1</sup>. The lowest SOC contents were found in the northern area, which corresponds to areas of greater anthropogenic intervention, while the highest SOC contents were located in the central and southern parts, which coincide with the least intervened area (Fig. 1B).

SOC contents at a depth of 15-30 cm were mainly less than 100 t ha<sup>-1</sup>, with a second significant group of samples between 150 and 300 t ha<sup>-1</sup> (Fig. 2A). The spatial distribution of SOC at 15-30 cm depth was similar to that at 0-15 cm (Fig. 2B). Lower contents were located in the northern part, and higher contents in the central and southern zones.

A



B

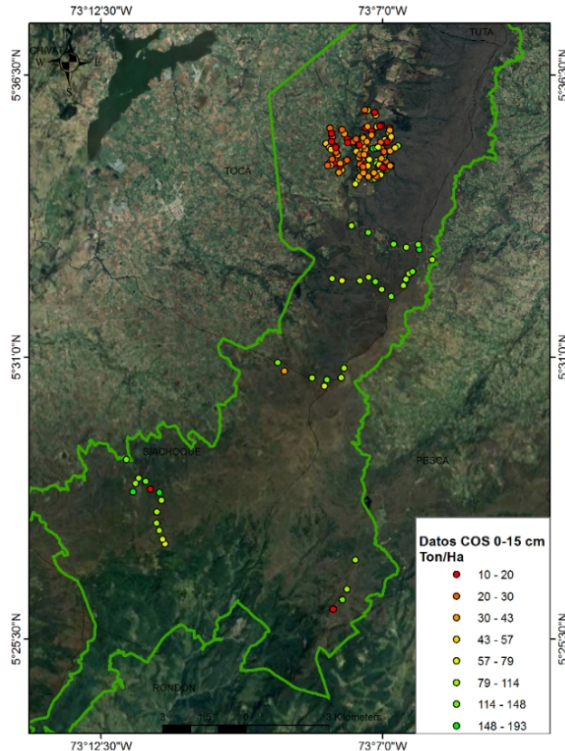
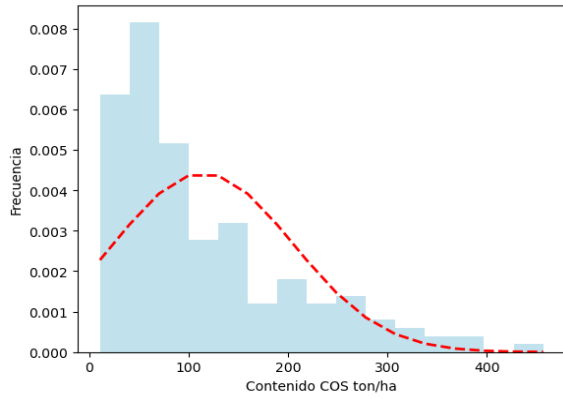


**FIGURE 1.** Soil organic carbon contents (A) and spatial distribution (B) at 0-15 cm depth.

A



B

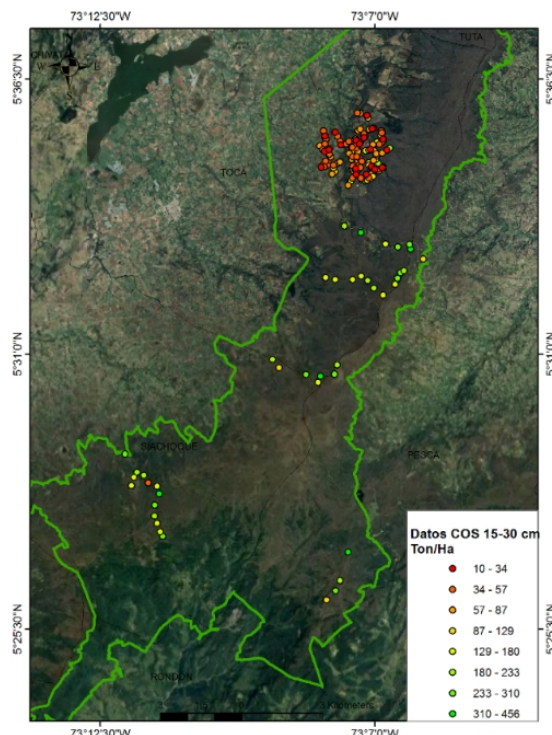


**FIGURE 2.** Soil organic carbon contents (a) and spatial distribution at 15-30 cm depth.

Gutiérrez *et al.* (2020) reported SOC contents in the paramos of Boyaca at a depth of 0-30 cm between 22 and 337 t ha<sup>-1</sup>. They noted that lower SOC contents correspond to areas with higher anthropogenic activity, mainly due to livestock and agricultural activity, which lead to greater mineralization of organic carbon through oxidation of organic matter (Burbano, 2018).

Correlations were significant at both depths for altitude, BSI, EVI, GNDVI, MRVBF, MSI, NBRI, NDVI, NDWI, AVI, temperature, and VH. Additionally, the TWI and LS factors showed significant correlations at a depth of 0-15 cm, while precipitation was significant at 15-30 cm (Tab. 1).

**TABLE 1. Correlation between soil organic carbon contents and spectral indices, DEM cartographic parameters and Worldclim climate data.**

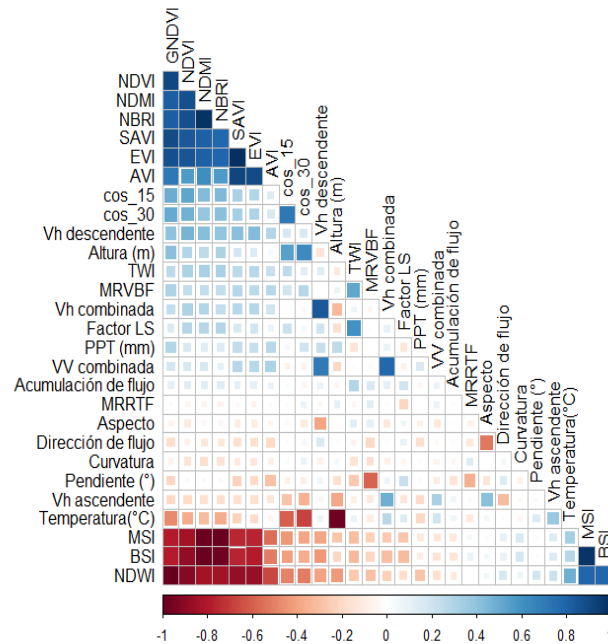
Parameter	Depth 15 cm	Significance	Depth 30 cm	Significance	VIF
Altitude	0.55	***	0.64	***	4.5
Aspect	-0.03		-0.1		5.2
SAVI	0.14		0.16		158
BSI	-0.41	***	-0.37	***	167
Curvature	0.02		0.08		1.5
EVI	0.29	***	0.3	***	199
Flow accumulation	0.02		-0.05		1.4
Flow direction	0.02		0.04		2.9
GNDVI	0.50	***	0.51	***	316
LS-factor	0.22	**	0.05		4.1
MRRTF	0.02		0.08		2.1
MRVBF	0.20	**	0.29	***	2.4
MSI	-0.43	***	-0.39	***	88
NBRI	0.45	***	0.41	***	118
NDMI	0.43	***	0.39	***	134
NDVI	0.52	***	0.48	***	20
NDWI	-0.50	***	-0.51	***	316
Precipitation	0.04		0.21	**	161
AVI	0.32	***	0.33	***	324
Slope	-0.08		-0.09		4.3
Temperature	-0.60	***	-0.67	***	4.7
TWI	0.26	***	0.12		5.1
VH	0.28	***	-0.34	***	669
VV	-0.07		-0.07		4.4

NDVI, Normalized Difference Vegetation Index; EVI, Enhanced Vegetation Index; BSI, Bare Soil Index; AVI, Advanced Vegetation Index; SAVI, Soil Adjusted Vegetation Index; GNDVI, Green Normalized Difference Vegetation Index; NDMI, Normalized Difference Moisture Index; MSI, Moisture Stress Index; NDWI, Normalized Difference Water Index; NBRI, Normalized Burn Ratio Index; MRVBF, Multiresolution Index of Valley Bottom Flatness; MrRTF, Multiresolution Index of the

Ridge Top Flatness; TWI, Topographic Wetness Index; LS-factor, slope length and steepness factor; VV, VH polarized data from SAR image. \*\*\*  $P < 0.99$ , \*\*  $P < 0.95$ , \*  $P < 0.90$ .

The highest correlation coefficients were found in most spectral indices, with NDVI having the highest at 0.52 at 0-15 cm and 0.47 at 15-30 cm. Among the DEM cartographic elements, altitude obtained the strongest correlations with 0.55 at 0-15 cm and 0.64 at 15-30 cm. Temperature showed significant correlations with -0.60 and -0.67 for depths of 0-15 and 15-30 cm, respectively (Fig. 3A). The spectral indices showed high VIF values due to the common base of the bands, explaining the high correlation. The collinearity analysis showed that NDVI, elevation, TWI0-15 cm, MRVBF, LS factor 0-15 cm, temperature, and VH band polarization had low VIF values (Fig. 3B).

A



B

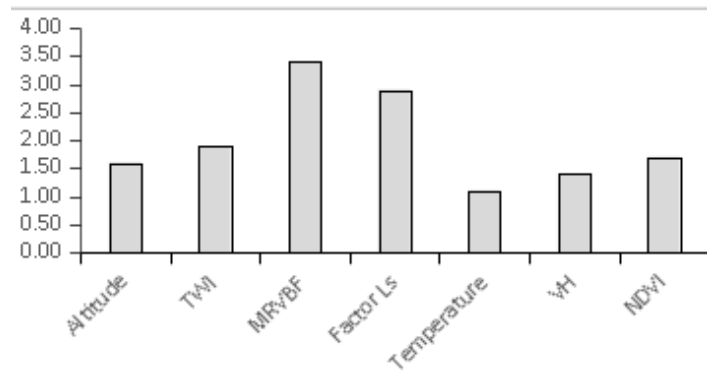
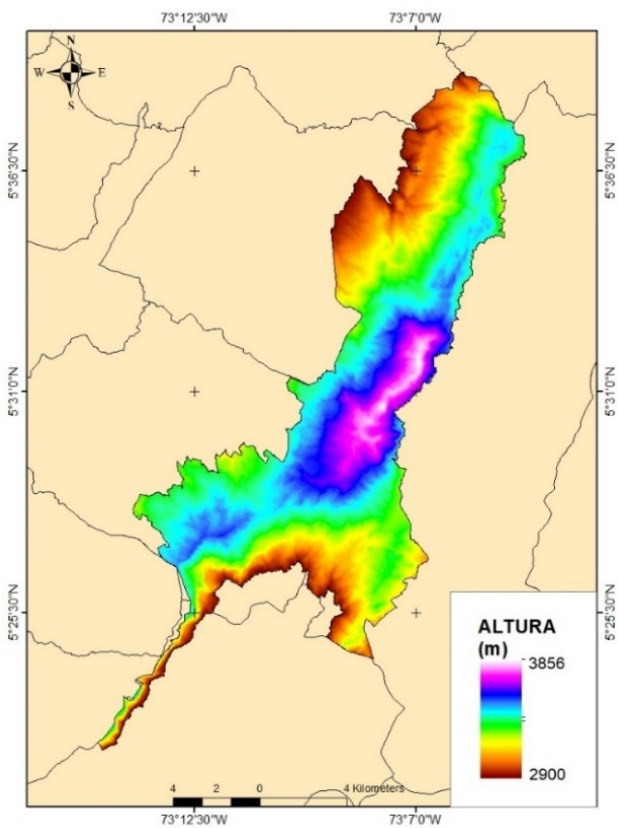


**FIGURE 3. Correlation and variance inflation factor of spectral indices, DEM cartographic parameters, and WorldClim climate data. See abbreviations in table 1.**

Based on the above, a more detailed spatial distribution analysis was conducted, revealing that the highest elevation areas are located in the central part, with a maximum elevation of 3,856 m. The southern and northern zones decrease to an elevation of 2,900 m (Fig. 4A). Given that there is a correlation between elevation and temperature, the latter being one of the factors affecting the decomposition and mineralization of organic matter, the higher altitude areas have higher SOC, consistent with observations by Quesada *et al.* (2020), Huamán-Carrión *et al.* (2021), and Hunt *et al.*

(2020), which indicate that as altitude increases, temperature decreases, and thus, the capacity for SOC storage increases.

A



B

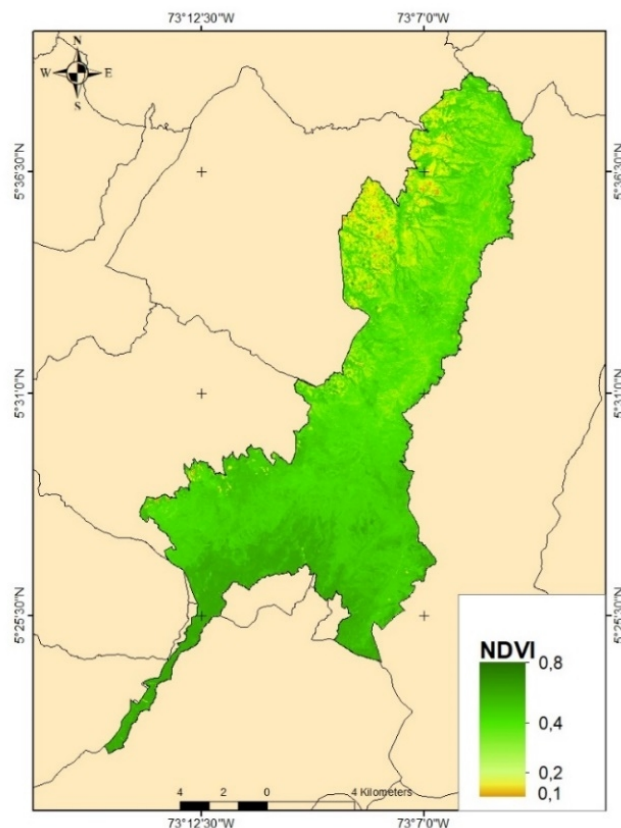


**FIGURE 4. Spatial variation of elevation (A) and NDVI (B).**

The relevance of elevation on soil organic carbon content is observed by Wang *et al.* (2018) in eastern Australia, who found that elevation is more significant for SOC content compared to other topographic elements such as aspect, slope, and TWI. Additionally, relief is among the most utilized parameters for predicting SOC (Chen *et al.*, 2022), as topographic elements are crucial for describing soil formation (Behrens *et al.*, 2010) and are more specifically used in estimating SOC (Wang *et al.*, 2018). Besides elevation, the LS factor also has an impact on SOC content, according to Reyes *et al.* (2018), who note that these topographic elements were significant in explaining SOC in a high Andean Mountain area, an ecosystem similar to the paramo.

Similarly, Davy and Koen (2013) explain that topography influences SOC storage by influencing soil depth and moisture, alongside other significant parameters such as TWI, LS factor, MRVBF, and

elevation. These factors are closely related to soil water and nutrient retention. Thus, areas with higher retention capacity facilitate plant growth, increasing organic matter inputs, which are the main constituent of SOC. In addition, these factors are fundamental in nutrient cycling, infiltration, and water retention capacity (Wang *et al.*, 2018). MRVBF is also relevant, as it identifies areas with potential deposition of eroded material, including organic matter (Chen *et al.*, 2022).

The NDVI values were lower in the northern zone (Fig. 4B), where there is less vegetation and corresponds to the buffer zone of the paramo with more agricultural intervention. Higher values were found in the southern zone, mainly corresponding to paramo shrubs. The importance of spectral indices lies in their use to determine the spatial variation of vegetation (Kuang *et al.*, 2015), as they represent vegetation type, which determines SOC storage (Yang *et al.*, 2018). Pastures and crops show low SOC values because anthropogenic activities strongly affect SOC storage, especially in this paramo ecosystem (Gutiérrez *et al.*, 2020).

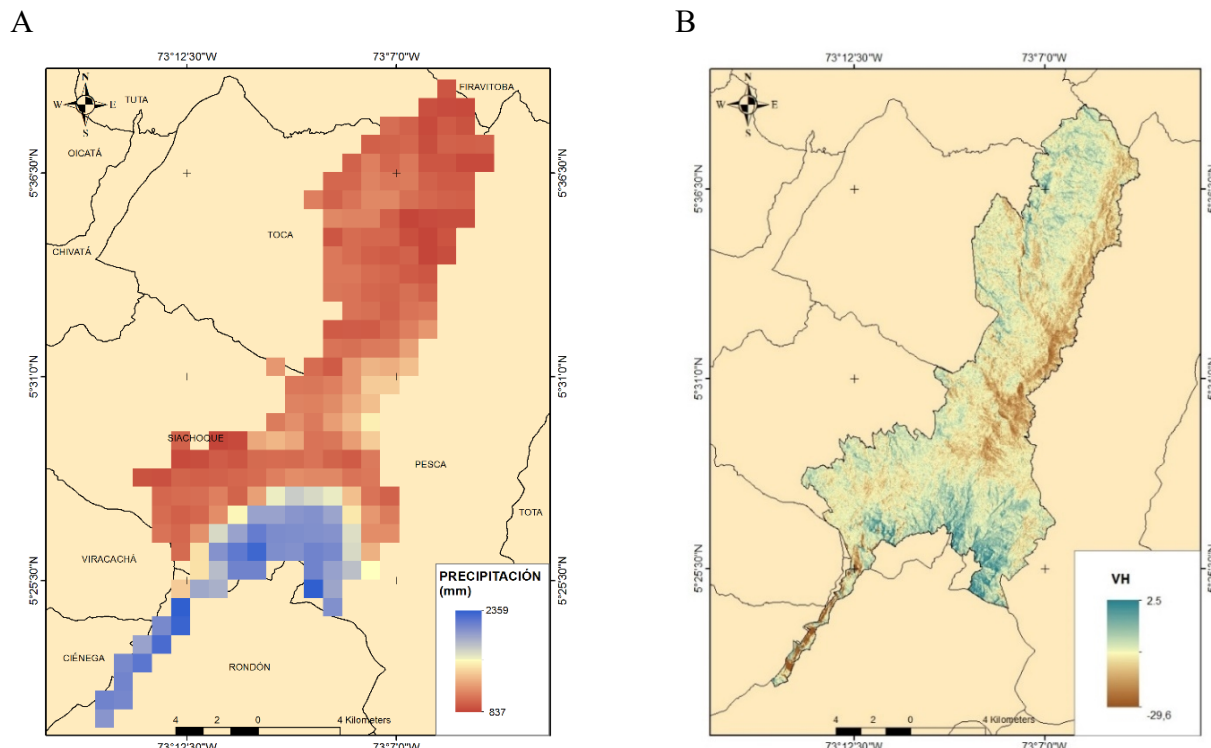


**FIGURE 5. Spatial distribution of precipitation and VH band.**

The correlation of spectral indices with SOC content, especially NDVI, suggests the usefulness of NVDI as an indicator of land cover (Wang *et al.*, 2017), considering its relationship with organic

material inputs (Waters *et al.*, 2015). Advances in remote sensing have contributed to carbon cycle knowledge, highlighting the importance of spectral indices in estimating and quantifying SOC (Xiao *et al.*, 2019). While our results align with these authors, spectral indices do not always provide good information, as they heavily depend on the study area and are unreliable when there is more than 20% bare soil (Sankey and Weber, 2009).

Climate data show differences in precipitation, with higher values in the southern zone (2,359 mm) and lower in the north (837 mm) (Fig. 5A). Precipitation differences (1,522 mm) determine vegetation type, organic matter decomposition rate, and SOC content (Wang *et al.*, 2014). Climates with high precipitation and low temperatures, such as paramos, facilitate SOC accumulation due to the inhibition of microorganisms to decompose organic matter (Buol *et al.*, 2011).

Temperature and precipitation showed significance, but with limited spatial resolution. Nevertheless, their relevance for this study aligns with Akpa *et al.* (2016), who indicated that climatic variables influence the rate of organic matter (OM) decomposition, determining quantity and quality in terrestrial systems.

The correlation of the VH band with SOC content identifies higher values in the southern zone and lower towards the north (Fig. 5B). This index is associated with soil moisture content (Hosseini and McNairn, 2017).

Zhou *et al.* (2020) used the VV/VH ratio from Sentinel-1, which, combined with information from Sentinel-2 and topographic variables, yields better explanatory results for SOC content compared to results using only spectral indices. It also shows better results than Landsat and Modis data.

## CONCLUSIONS

Remote sensing allowed the estimation of soil organic carbon content using topographic elements, spectral indices, and climate data. The LS factor, TWI, MRVBF, elevation, and VH band were the most significant among topographic elements, NDVI among spectral indices, and temperature and precipitation among climate variables. Higher soil organic carbon contents were found in areas with higher elevation, greater precipitation, lower temperature, and less anthropogenic intervention.

## Acknowledgements

This article is part of the research work developed for the master's thesis "Method for Estimating the Spatial Distribution of Organic Carbon Content in Páramo Soil Based on Remote Sensing Data," National University of Colombia.

**Conflict of interests:** The manuscript was prepared and reviewed with the participation of the authors, who declare that there exists no conflict of interest that puts at risk the validity of the presented results.

## LITERATURE CITED

Africano, K.L. G.E. Cely, and P.A. Serrano. 2016. Potencial de captura de CO<sub>2</sub> asociado al componente edáfico en páramos Guantiva-La Rusia, departamento de Boyacá, Colombia. Perspect. Geogr. 21(1), 91-110.

Akpa, S.I.C., I.O.A. Odeh, T.F.A. Bishop, A.E. Hartemink, and I.Y. Amapu. 2016. Total soil organic carbon and carbon sequestration potential in Nigeria. Geoderma 271, 202-215. Doi: <https://doi.org/10.1016/j.geoderma.2016.02.021>

Andrade, H.J., M.A. Segura, and D.S. Canal-Daza. 2022. Conservation of soil organic carbon in the national park Santuario de Fauna y Flora Iguaque, Boyacá-Colombia. Forests 13(8), 1275. Doi: <https://doi.org/10.3390/f13081275>

Armas, D., M. Guevara, D. Alcaraz-Segura, R. Vargas, M.A. Soriano-Luna, P. Durante, and C. Oyonarte. 2017. Mapa digital del perfil del carbono orgánico en los suelos de Andalucía, España. Ecosistemas 26(3), 80-88. Doi: <https://doi.org/10.7818/ECOS.2017.26-3.10>

Ayala, J.E. 2019. Mapeo digital de carbono orgánico del suelo mediante imágenes satelitales y algoritmos de autoaprendizaje en el ecosistema Herbazal del Páramo, provincia de Chimborazo, Ecuador. MSc thesis. Facultad de Ciencias Astronómicas y Geofísicas, Universidad Nacional de La Plata, Buenos Aires.

Ayala, L., M. Villa, Z. Aguirre, and N. Aguirre. 2014. Cuantificación del carbono en los páramos del parque nacional Yacuri, provincias de Loja y Zamora Chinchipe, Ecuador. Rev. Cedamaz 4(1), 45-52.

Barrezueta-Unda, S., K.A. Velepucha-Cuenca, L. Hurtado-Flores, and E.E. Jaramillo-Aguilar. 2019. Soil properties and storage of organic carbon in the land use pasture and forest. Rev. Cienc. Agric. 36(2), 31-45. Doi: <https://doi.org/10.22267/rcia.193602.116>

Behrens, T., A.-X. Zhu, K. Schmidt, and T. Scholten. 2010. Multi-scale digital terrain analysis and feature selection for digital soil mapping. Geoderma 155(3-4), 175-185. Doi: <https://doi.org/10.1016/j.geoderma.2009.07.010>

Buol, S.W., R.J. Southard, R.C. Graham, and P.A. McDaniel. 2011. Soil genesis and classification. 6<sup>th</sup> ed. John Wiley & Sons, Chichester, UK. Doi: <https://doi.org/10.1002/9780470960622>

Burbano, H. 2018. El carbono orgánico del suelo y su papel frente al cambio climático. Rev. Cienc. Agric. 35(1), 82-86. Doi: <https://doi.org/10.22267/rcia.183501.85>

Canaza, D., E. Calizaya, W. Chambi, F. Calizaya, C. Mindani, O. Cuentas, C. Caira, and W. Huacani. 2023. Spatial distribution of soil organic carbon in relation to land use, based on the weighted overlay technique in the High Andean ecosystem of Puno—Peru. Sustainability 15(13), 10316. Doi: <https://doi.org/10.3390/su151310316>

Carrillo-Rojas, G., B. Silva, R. Rollenbeck, R. Céller, and J. Bendix. 2019. The breathing of the Andean highlands: Net ecosystem exchange and evapotranspiration over the páramo of southern Ecuador. Agric. Forest Meteorol. 265, 30-47. Doi: <https://doi.org/10.1016/j.agrformet.2018.11.006>

Chen, S., D. Arrouays, V. Leatitia Mulder, L. Poggio, B. Minasny, P. Roudier, Z. Libohova, P. Lagacherie, Z. Shi, J. Hannam, J. Meersmans, A.C. Richer-de-Forges, and C. Walter. 2022. Digital mapping of *GlobalSoilMap* soil properties at a broad scale: a review. Geoderma 409, 115567. Doi: <https://doi.org/10.1016/j.geoderma.2021.115567>

Corporinoquia, Corporación Autónoma Regional de la Orinoquía. 2017. Estudio técnico, económico, social y ambiental para la identificación y delimitación del complejo de páramos de Pisba (Report). Fundación Orinoquía Biodiversa, Yopal, Colombia.

Cuervo-Barahona, E.L., G.E. Cely-Reyes, and D.F. Moreno-Pérez. 2016. Determinación de las fracciones de carbono orgánico en el suelo del páramo La Cortadera, Boyacá. Ingenio Magno 7(2), 139-149.

Davy, M.C. and T.B. Koen. 2013. Variations in soil organic carbon for two soil types and six land uses in the Murray Catchment, New South Wales, Australia. Soil Res. 51(8), 631-644. Doi: <https://doi.org/10.1071/SR12353>

FAO. 2017. Carbono orgánico del suelo: el potencial oculto. Rome.

Gardi, C., M. Angelini, S. Barceló, J. Comerma, C. Cruz Gaistardo, A. Encina Rojas, A. Jones, P. Krasilnikov, M.L.M.S. Brefin, L. Montanarella, O. Muñiz Ugarte, P. Schad, M.I. Vara Rodríguez, and R. Vargas (eds.). 2014. Atlas de suelos de América Latina y el Caribe. L-2995. Comisión Europea, Oficina de Publicaciones de la Unión Europea, Luxembourg.

Gutiérrez, J., N. Ordoñez, A. Bolívar, S. Bunning, M. Guevara, E. Medina, C. Olivera, G. Olmedo, L.M. Rodríguez, V. Sevilla, and R. Vargas. 2020. Estimación del carbono orgánico en los suelos de ecosistema de páramo en Colombia. Ecosistemas 29(1), 1855. Doi: <https://doi.org/10.7818/ECOS.1855>

Hosseini, M. and H. McNairn. 2017. Using multi-polarization C-and L-band synthetic aperture radar to estimate biomass and soil moisture of wheat fields. Int. J. Appl. Earth Observ. Geoinform. 58, 50-64. Doi: <https://doi.org/10.1016/j.jag.2017.01.006>

Huamán-Carrión, M.L., F. Espinoza-Montes, A.I. Barrial-Lujan, and Y. Ponce-Atencio. 2021. Influencia de la altitud y características del suelo en la capacidad de almacenamiento de carbono orgánico de pastos naturales altoandinos. Sci. Agropecu. 12(1), 83-90. Doi: <https://doi.org/10.17268/SCI.AGROPECU.2021.010>

Hunt, J.R., C. Celestina, and J.A. Kirkegaard. 2020. The realities of climate change, conservation agriculture and soil carbon sequestration. *Global Change Biol.* 26(6), 3188-3189 Doi: <https://doi.org/10.1111/gcb.15082>

Kuang, B., Y. Tekin, and A.M. Mouazen. 2015. Comparison between artificial neural network and partial least squares for on-line visible and near infrared spectroscopy measurement of soil organic carbon, pH and clay content. *Soil Till. Res.* 146(Part B), 243-252. Doi: <https://doi.org/10.1016/j.still.2014.11.002>

Lis-Gutiérrez, M., Y. Rubiano-Sanabria, and J.C. Loaiza-Usuga. 2019. Soils and land use in the study of soil organic carbon in Colombian highlands catena. *AUC Geograph.* 54(1), 15-23. Doi: <https://doi.org/10.14712/23361980.2019.2>

Moreno, F., S.F. Oberbauer, and W. Lara. 2017. Soil organic carbon sequestration under different tropical cover types in Colombia. pp. 367-383. In: Bravo, F., V. LeMay, and R. Jandl (eds.). *Managing forest ecosystems: the challenge of climate change.* Vol. 34: managing forest ecosystems. Springer, Cham, Switzerland. Doi: [https://doi.org/10.1007/978-3-319-28250-3\\_18](https://doi.org/10.1007/978-3-319-28250-3_18)

Montes-Pulido, C.R., J.J. Ramos, and A.M. San José Wery. 2017. Estimation of soil organic carbon (SOC) at different soil depths and soil use in the Sumapaz paramo, Cundinamarca - Colombia. *Acta Agron.* 66(1), 95-101. Doi: <https://doi.org/10.15446/acag.v66n1.53171>

Morales, M., J. Otero, T. Van Der Hammen, A. Torres, C. Cadena, C. Pedraza, N. Rodríguez, C. Franco, J.C. Betancourth, E. Olaya, E. Posada, and L. Cárdenas. 2007. *Atlas de páramos de Colombia.* Instituto de Investigación de Recursos Biológicos Alexander von Humboldt. Bogota.

Quesada, C.A., C. Paz, E. Oblitas Mendoza, O.L. Phillips, G. Saiz, and J. Lloyd. 2020. Variations in soil chemical and physical properties explain basin-wide Amazon forest soil carbon concentrations. *SOIL* 6(1), 53-88. Doi: <https://doi.org/10.5194/soil-6-53-2020>

Reyes, L.A., K. Adhikari, and S.J. Ventura. 2018. Projecting soil organic carbon distribution in Central Chile under future climate scenarios. *J. Environ. Qual.* 47(4), 735-745. Doi: <https://doi.org/10.2134/jeq2017.08.0329>

Rügnitz, M., M. Chacón, and R. Porro. 2009. Guía para la determinación de carbono en pequeñas propiedades rurales. Centro Mundial Agroflorestal (ICRAF); Consorcio Iniciativa Amazónica (IA), Lima.

Sankey, T.T. and K. Weber. 2009. Rangeland assessments using remote sensing: is NDVI useful? pp. 113-122. In: Weber, K.T. and K. Davis (eds.). Comparing effects of management practices on rangeland health with geospatial technologies. Report NNX06AE47G. Idaho State University, Pocatello, ID.

Wang, X., E.L.H. Cammeraat, C. Cerli, and K. Kalbitz. 2014. Soil aggregation and the stabilization of organic carbon as affected by erosion and deposition. *Soil Biol. Biochem.* 72, 55-65. Doi: <https://doi.org/10.1016/j.soilbio.2014.01.018>

Wang, B., C. Waters, S. Orgill, J. Gray, A. Cowie, A. Clark, and D.L. Liu. 2018. High resolution mapping of soil organic carbon stocks using remote sensing variables in the semi-arid rangelands of eastern Australia. *Sci. Total Environ.* 630, 367-378. Doi: <https://doi.org/10.1016/j.scitotenv.2018.02.204>

Wang, S., Q. Zhuang, Q. Wang, X. Jin, and C. Han. 2017. Mapping stocks of soil organic carbon and soil total nitrogen in Liaoning Province of China. *Geoderma* 305, 250-263. Doi: <https://doi.org/10.1016/j.geoderma.2017.05.048>

Ward, A., P. Dargusch, G. Grussu, and R. Romeo. 2016. Using carbon finance to support climate policy objectives in high mountain ecosystems. *Clim. Policy* 16(6), 732-751. Doi: <https://doi.org/10.1080/14693062.2015.1046413>

Waters, C.M., G.J. Melville, S.E. Orgill, and Y. Alemseged. 2015. The relationship between soil organic carbon and soil surface characteristics in the semi-arid rangelands of southern Australia. Rangel. J. 37(3), 297-307. Doi: <https://doi.org/10.1071/RJ14119>

Xiao, J., F. Chevallier, C. Gomez, L. Guanter, J.A. Hicke, A.R. Huete, K. Ichii, W. Ni, Y. Pang, A.F. Rahman, G. Sun, W. Yuan, L. Zhang, and X. Zhang. 2019. Remote sensing of the terrestrial carbon cycle: a review of advances over 50 years. Remote Sens. Environ. 233, 111383. Doi: <https://doi.org/10.1016/j.rse.2019.111383>

Yang, S., D. Sheng, J. Adamowski, Y. Gong, J. Zhang, and J. Cao. 2018. Effect of land use change on soil carbon storage over the last 40 years in the Shi Yang River Basin, China. Land 7(1), 11. Doi: <https://doi.org/10.3390/land7010011>

Zhou, T., Y. Geng, J. Chen, J. Pan, D. Haase, and A. Lausch. 2020. High-resolution digital mapping of soil organic carbon and soil total nitrogen using DEM derivatives, Sentinel-1 and Sentinel-2 data based on machine learning algorithms. Sci. Total Environ. 729, 138244. Doi: <https://doi.org/10.1016/j.scitotenv.2020.138244>

Zimmermann, M., P. Meir, M.R. Silman, A. Fedders, A. Gibbon, Y. Malhi, D.H. Urrego, M.B. Bush, K.J. Feeley, K.C. Garcia, G.C. Dargie, W.R. Farfan, B.P. Goetz, W.T. Johnson, K.M. Kline, A.T. Modi, N.M.Q. Rurau, B.T. Staudt, and F. Zamora. 2010. No differences in soil carbon stocks across the tree line in the Peruvian Andes. Ecosystems 13(1), 62-74. Doi: <https://doi.org/10.1007/s10021-009-9300-2>

Zuur, A.F., E.N. Ieno, and G.M. Smith. 2007. Analysing ecological data. Springer, New York, NY. Doi: <https://doi.org/10.1007/978-0-387-45972-1>